Diamond & Related Materials 57 (2015) 9–16

Contents lists available at ScienceDirect

Diamond & Related Materials

journal homepage: www.elsevier.com/locate/diamond

Features of free carrier and exciton recombination, diffusion, and photoluminescence in undoped and phosphorus-doped diamond layers

P. Ščajev [a,*], J. Jurkevičius [a], J. Mickevičius [a], K. Jarašiūnas [a], H. Kato [b]

[a] Institute of Applied Research, Vilnius University, LT-10222 Vilnius, Lithuania
[b] Energy Technology Research Institute, AIST 1-1-1 Umezono, Tsukuba, Ibaraki 305-8568, Japan

ARTICLE INFO

Available online 11 February 2015

Keywords:
Diffusion
Recombination
Luminescence
Excitons
Free carriers
Pump-probe techniques

ABSTRACT

We investigated carrier dynamics and photoluminescence in undoped and n-type phosphorus-doped diamond epilayers under interband picosecond-pulse photoexcitation at 213 nm. Carrier/exciton lifetime and diffusion coefficient D were determined in 4×10^{17} to 4×10^{19} cm^{-3} carrier density range. The low $D = 7 \div 11$ cm^2/s value in the undoped epilayer was ascribed to exciton formation and contribution of many-body effects. At low excitations, photoluminescence spectra in the undoped layer exhibited exciton emission, while at the higher ones (above 2×10^{18} cm^{-3}) free carrier emission became dominant. The calculated radiative lifetime of excitons (860 ns) was found much higher than the experimentally measured nonradiative lifetime of 11 ns, governed by excess carrier diffusive flow to the surface, with $S = (3 \pm 2) \times 10^5$ cm/s surface recombination velocity. In the n-type layer, donor-related emission dominated and the phosphorus-related defect complexes diminished the carrier lifetime to 30–50 ps. Optically recharged phosphorus states resulted in millisecond long decay tails of trapped carriers.

© 2015 Elsevier B.V. All rights reserved.

1. Introduction

Recently, the measured long lifetime value of 700–800 ns [1,2] and high photoluminescence efficiency (13% at 300 K for 10^{17} cm^{-3} carrier density [3]) in thick undoped CVD diamond confirmed its potential applications for high output p–i–n UV emitters at 235 nm [4,5]. Nevertheless, for practical applications of thin undoped diamond layers, impact of surface recombination has to be carefully studied. For n-type diamond films, doping by phosphorus (P) with rather high activation energy (0.65 eV [6]) leads to highly resistive layers with rather low mobility (e.g. equilibrium carrier density $n_0 = 10^{10}$ cm^{-3}, electron mobility $\mu_e =$ 100 cm^2/Vs at 300 K for ~2×10^{18} cm^{-3} phosphorus-doped layers [7]). The higher Hall mobility was achieved in low compensated *n*-type diamond ($\mu_e = 1000$ cm^2/Vs [8]) still being two times lower than the typical electron mobility in undoped diamond [9]. In spite of phosphorus activation energy reduced to 0.43 eV at high doping (2×10^{19} cm^{-3} [10]), the fabrication of high electronic quality n-type diamond is still a challenge.

Therefore, in the present work, we investigated carrier dynamics and photoluminescence spectra in undoped and n-type phosphorus-doped epilayers by using interband photoexcitation by picosecond laser pulses at 213 nm. Light-induced transient grating (LITG), differential transmittivity (DT), and time integrated photoluminescence (TIPL) techniques were applied for determination of key electronic parameters of thin diamond layers.

2. Sample and experimental techniques

We investigated undoped and n-type phosphorus-doped (2.3×10^{18} cm^{-3}) epilayers grown on high temperature high pressure (HPHT) Ib (001) substrates. The layers were 10 and 2.7 μm thick, respectively. The sample growth details can be found in [7]. In the P-doped sample, only 6.6×10^{17} cm^{-3} of phosphorus was in its single substitutional state, whereas quite strong compensation was evident from N_D–$N_A = 2.3 \times 10^{17}$ cm^{-3} value. Compensating centers were attributed to hydrogen complex with carbon vacancies (HV_C) at $E_C - (1.2$–$1.4)$ eV, with a density of 4.3×10^{17} cm^{-3}. The other part of P would be complexed with hydrogen or vacancies.

For investigation of carrier diffusion and recombination, the optical pump-probe techniques were applied. The Nd:YAG laser emitting at 213 nm (15 ps duration pulses and 10 Hz repetition rate) was used to generate excess carriers. The delayed infrared pulse (at 1064 nm) from the same laser was probing the induced absorption by photogenerated carriers [11] or light diffraction on the light-induced free-carrier grating (LITG) [12]. In the latter case, the spatial modulation with period Λ was recorded by interference pattern of two intersecting excitation beams. The excess carrier density was described by $\Delta N(x) = \Delta N_0[1 + \cos(2\pi x / \Lambda)] \times \exp(-\alpha_{213} z)$ relationship, where $\Delta N_0 = \alpha_{213} I_0 / E_{213}$ is the carrier density near the excited surface; α_{213} is the interband absorption coefficient at 213 nm, equal to 3500 cm^{-1} as

* Corresponding author.
E-mail address: patrik.scajev@ff.vu.lt (P. Ščajev).

http://dx.doi.org/10.1016/j.diamond.2015.02.003
0925-9635/© 2015 Elsevier B.V. All rights reserved.

measured by diffraction based technique [13], $E_{213} = 5.82$ eV is the pump quantum energy, x and z are the in-plane and in-depth coordinates, and I_0 is the excitation fluence. The instantaneous probe beam diffraction efficiency on a grating, $\eta \sim \Delta N_0^2 \exp(-2t/\tau_G)$ and its decay provided the grating decay times τ_G at different Λ. The carrier diffusion coefficient D and short lifetime ($\tau_R < 5$ ns) were determined according to the $1/\tau_G = 1/\tau_R + 4\pi^2 D/\Lambda^2$ relationship [14]. Average carrier density shortly after the excitation was estimated by $\Delta N = \Delta N_0/2$ relationship [15].

Differential transmittivity (DT) decay was monitored for determination of carrier lifetime values τ_R (in the range from 20 ps to microseconds) at various excitations. Two kinds of time-delayed probe pulses were used [16]. The optically delayed (<4 ns) 25 ps duration probe pulse at 1064 nm was used to monitor the fast decay transients (<10 ns). For measurement of longer relaxation decays (>5 ns), an electronically delayed ~2 ns duration probe pulse at 1064 nm was obtained from a nanosecond Nd:YAG laser, triggered by the picosecond Nd:YLF laser [16]. Combining the optical and electronic delay of the probe beam, we investigated both the fast (up to tens of ns) and slow (up to hundreds of μs) recombination transients. The DT signal is described by a relation [16]: $DT = \ln(T_0/T(t)) = \sigma_{eh}\int_0^d \Delta N(z,t)dz$. Here $\sigma_{eh} = \sigma_e + \sigma_h$ is the free carrier absorption (FCA) cross section, consisting of electron, σ_e, and hole, σ_h, absorption cross sections [11,17] (for probing excitons well below the diamond bandgap (at 1.17 eV) this relationship must also be valid [18]); T_0 and $T(t)$ are the sample transmissions for probe wavelength without excitation and under excitation, respectively. In the case when electrons and holes recombine independently (e.g. nitrogen or phosphorus trap density is larger than ΔN_0), a relation $\ln(T_0/T(t)) = \int_0^d \sigma_e \Delta N_e(z,t) + \sigma_h \Delta N_h(z,t) + \sigma_t \Delta N_t(z,t)dz$ has to be used, where ΔN_e, ΔN_h and ΔN_t are the excess electron, hole and recharged trap (with absorption cross section σ_t) densities, respectively.

The time-integrated PL (TIPL) spectra were measured using the 5th harmonic (213 nm) of a Q-switched Nd:YAG laser (with 4 ns pulse duration) for excitation. The PL signal was analyzed using a double grating monochromator (Jobin Yvon HRD-1) and recorded by a photomultiplier tube and a boxcar integrator. Spectral resolution was 16 meV.

3. Experimental results

3.1. Diffusion coefficient excitation dependence in the undoped layer

For determination of D by LITG technique, we performed grating decay measurements at small and large grating periods (1.72 μm and 6.8 μm). The grating decay for small period (Fig. 1a) was almost exponential and diffusion limited, i.e. $\tau_G \approx \Lambda^2/4\pi^2 D < 100$ ps, while the recombination decay time was much longer, $\tau_R > 1$ ns (see Fig. 2b). Therefore, measurements of grating diffusive decay at various excitations (Fig. 1a) provided $D(\Delta N)$ dependence on generated electron–hole pair density $\Delta N = \Delta N_h = \Delta N_e$ (Fig. 1b). We note, that the total carrier density (ΔN) consists of exciton (ΔN_{ex}) and free carrier (ΔN_{FC}) concentrations: $\Delta N = \Delta N_{ex} + \Delta N_{FC}$. The observed strong decrease of diffusion coefficient with excess carrier density corresponds to conditions when relative exciton-to-total-carrier density ratio ($f_{ex}(\Delta N) = \Delta N_{ex}/\Delta N$) starts to increase.

As diamond has a very large exciton binding energy (80 meV), exciton formation at high enough excitations will provide not free carrier, but exciton diffusion coefficient. In Fig. 1b the relative ratio of exciton-to-total carrier density is presented. The exciton density was calculated according to $\Delta N_{ex} = \Delta N_{FC}^2/n^*$, $n^* = N_{dos\ ex}\exp(-E_{ex}(\Delta N_{FC})/k_B T)$ relations, where $N_{dos\ ex} = 2(2\pi m_{eh} k_B T/h^2)^{3/2} = 2.1 \times 10^{18}$ cm^{-3} (at 300 K) is the density of exciton states, $E_{ex}(\Delta N_{FC}) = E_{ex}(1 - [\Delta N_{FC}/N_{Mott}]^{1/4})$ [20] is the excitation dependent exciton binding energy (its dependence on carrier density was calculated using band-gap renormalization (BGR) by free carriers with density $\Delta N_{FC} = \Delta N - \Delta N_{ex}$), $N_{Mott} = 4 \times 10^{18}$ cm^{-3} is the exciton Mott transition density [21], $E_{ex} = 13.6$ eV $\times\, m_{eh} m_0^{-1} \varepsilon_s^{-2} =$ 80 meV is the exciton binding energy in hydrogenic approximation [20],

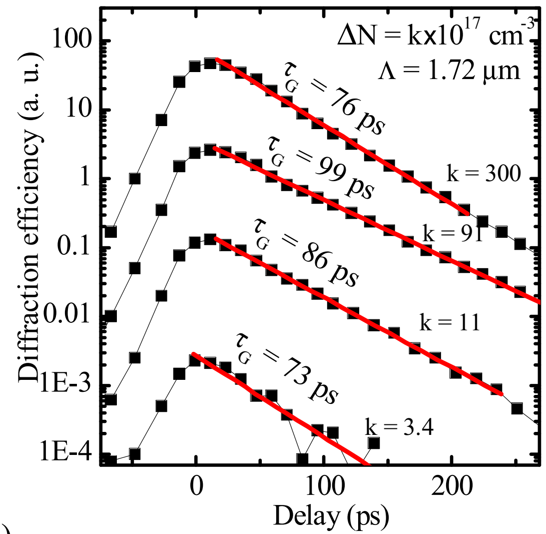

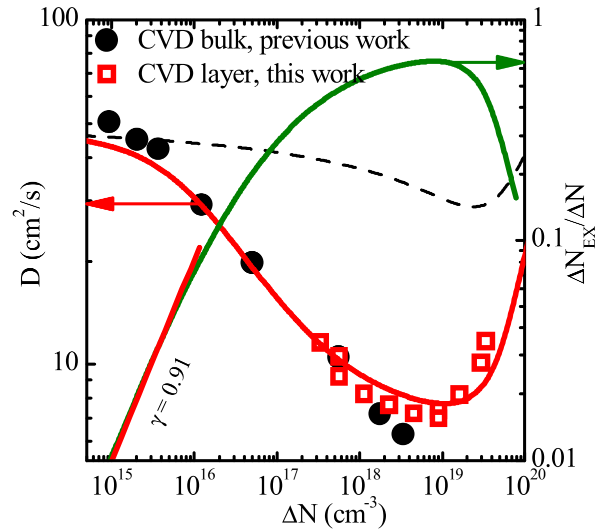

Fig. 1. Diffusive decay of LITG in undoped sample at various excitation levels (a) and the dependences of measured diffusion coefficient D and exciton-to-total carrier density ratio on the excess carrier density ΔN (b). Thick solid lines in (b) indicate the fit of diffusion coefficient. The dashed line presents the calculated $D_{FC}(\Delta N_{FC})$ dependence for free carriers, taking into account band gap renormalization and degeneracy effects. D values for an undoped bulk diamond (filled circles) were taken from [19]. Here γ is the slope value of the ratio dependence on excitation in the log–log plot, i.e. the index of the power dependence $Y = X^{\gamma}$.

and $\varepsilon_s = 5.7$ is the diamond static dielectric constant [6]. The E_{ex} relation provides $m_{eh} = 0.19\ m_0$. The value coincides with the calculated one in [22]. In the latter reference, $m_e^* = 0.385\ m_0$ is provided, what leads, according to $1/m_{eh} = 1/m_e^* + 1/m_h^*$ relationship, to $m_h^* = 0.375\ m_0$. Thus $m_e^* \approx m_h^*$ and therefore similar electron and hole mobilities were observed [9] as they are determined by carrier masses [18]. The calculations pointed out that at $\Delta N > 10^{17}$ cm^{-3} the exciton density (as well as the ratio $f_{ex}(\Delta N) = \Delta N_{ex}/\Delta N$) starts to saturate (Fig. 1b), while in 10^{18-19} cm^{-3} range it is almost constant. At higher excitations, excitons start to dissociate due to the Mott transition.

The calculations of an average diffusion coefficient for a mixed free carrier and exciton system were performed, using the equation

$$1/D = [\Delta N_{FC}/\Delta N]/D_{FC}(\Delta N_{FC}) + [\Delta N_{ex}/\Delta N]/D_{EX}, \quad (1)$$

assuming additive scattering rates of free carriers and excitons (here $D_{FC}(\Delta N_{FC})$ and D_{EX} are free-carrier and exciton diffusion coefficients,

Download English Version:

https://daneshyari.com/en/article/701540

Download Persian Version:

https://daneshyari.com/article/701540

Daneshyari.com